Biodegradable Gelatin Methacryloyl Microneedles for Transdermal Drug Delivery

Zhimin Luo,

Department of Bioengineering, University of California-Los Angeles, Los Angeles, CA 90095, USA; School of Pharmacy, Xi'an Jiaotong University, Xi'an 710061, China; Center for Minimally Invasive Therapeutics (C-MIT), California NanoSystems Institute, University of California-Los Angleles, Los Angeles, CA 90095, USA; Key Laboratory of Tibetan Medicine Research, Northwest Institute of Plateau Biology, Chinese Academy of Sciences, Xining, 810001, China

Wujin Sun[*],

Department of Bioengineering, University of California-Los Angeles, Los Angeles, CA 90095, USA; Center for Minimally Invasive Therapeutics (C-MIT), California NanoSystems Institute, University of California-Los Angleles, Los Angeles, CA 90095, USA

Jun Fang,

Department of Bioengineering, University of California-Los Angeles, Los Angeles, CA 90095, USA

KangJu Lee,

Department of Bioengineering, University of California-Los Angeles, Los Angeles, CA 90095, USA; Center for Minimally Invasive Therapeutics (C-MIT), California NanoSystems Institute, University of California-Los Angleles, Los Angeles, CA 90095, USA

Song Li,

Department of Bioengineering, University of California-Los Angeles, Los Angeles, CA 90095, USA; Department of Medicine, University of California-Los Angeles, Los Angeles, CA 90095, USA

Zhen Gu,

Department of Bioengineering, University of California-Los Angeles, Los Angeles, CA 90095, USA; Center for Minimally Invasive Therapeutics (C-MIT), California NanoSystems Institute, University of California-Los Angleles, Los Angeles, CA 90095, USA

Mehmet R. Dokmeci, and

Department of Bioengineering, University of California-Los Angeles, Los Angeles, CA 90095, USA; Center for Minimally Invasive Therapeutics (C-MIT), California NanoSystems Institute, University of California-Los Angleles, Los Angeles, CA 90095, USA; Department of Chemical and Biomolecular Engineering, University of California-Los Angeles, Los Angeles, CA 90095, USA

Ali Khademhosseini[*]

Department of Bioengineering, University of California-Los Angeles, Los Angeles, CA 90095, USA; Center for Minimally Invasive Therapeutics (C-MIT), California NanoSystems Institute,

[*] sunwj@ucla.edu; khademh@ucla.edu.

University of California-Los Angleles, Los Angeles, CA 90095, USA; Jonsson Comprehensive Cancer Center, University of California - Los Angeles, 10833 Le Conte Ave, Los Angeles, CA 90024, USA; Department of Chemical and Biomolecular Engineering, University of California-Los Angeles, Los Angeles, CA 90095, USA; Department of Radiology, University of California-Los Angeles, Los Angeles, CA 90095, USA; Center of Nanotechnology, Department of Physics, King Abdulaziz University, Jeddah 21569, Saudi Arabia; Department of Bioindustrial Technologies, College of Animal Bioscience and Technology, Konkuk University, Seoul, Republic of Korea

Abstract

Biocompatible and bioresponsive microneedles (MNs) are emerging technology platforms for sustained drug release with a potential to be a key player in transdermal delivery of therapeutics. In this paper, we report an innovative biodegradable MNs patch for the sustained delivery of drugs using a polymer patch which can adjust delivery rates based on its crosslinking degree. Gelatin methacryloyl (GelMA) was used as the base for engineering biodegradable MNs. The anticancer drug Doxorubicin (DOX) was loaded into GelMA MNs using the one molding step. The GelMA MNs could efficiently penetrate the *stratum corneum* layer of a mouse cadaver skin. Mechanical properties and drug release behavior of the GelMA MNs could be adjusted by tuning the degree of crosslinking. We have tested the efficacy of the DOX released from the GelMA MNs and demonstrated the anticancer efficacy of the released drugs against melanoma cell line A375. Since GelMA is versatile material in engineering tissue scaffolds, we expect that the GelMA MNs could be used as a platform for the delivery of various therapeutics.

Graphical Abstract

A biocompatible and biodegradable microneedles patch based on gelatin methacryloyl was developed for transcutaneous delivery of drugs. The microneedles could efficiently penetrate the *stratum corneum* layer in a mouse cadaver skin model and the drug release profile could be controlled by tuning the crosslinking degrees. The model drug Doxorubicin kept its anticancer efficacy after enzyme-mediated release from the patch.
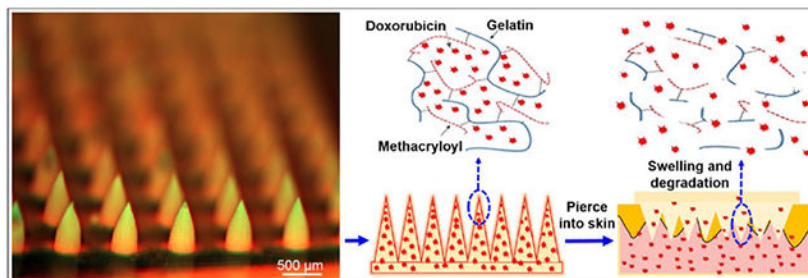
Keywords

transdermal drug delivery; microneedle; gelatin methacryloyl; sustained release

Skin is the largest organ of the human body that takes approximately 15% of total body weight. It is composed of multiple layers including epidermis, dermis, and hypodermis.[1] The outermost layer of the epidermis, *stratum corneum*, functions as the skin barrier, which

also limits the availability of therapeutics for target areas beneath the epidermis.[2] Compared with traditional hypodermic needle based drug delivery, MNs are small enough not to be visible to the naked eye and hence are friendly to patients with needle phobia.[3] Compared with sonophoresis or iontophoresis-based transdermal drug delivery that needs dedicated electronic devices,[4] MN patches are easy to apply without the prerequisite of requiring complex devices.[5] Due to their microscale dimensions MNs can puncture the skin seamlessly and can deliver a range of therapeutic molecules including ones with a wide range of molecular weights, such as small molecules, biomacromolecules, and even nanoparticles.[6] Compared with chemical formulations for enhanced transdermal drug delivery, such as lipid nanoparticles, manufacturing the MNs requires much lower cost and has a high batch to batch reproducibility.[7] In the meantime, the depth of the MNs penetration could be arranged to solely penetrate the epidermis without damaging neurons in the dermis, minimizing the pain associated with transdermal drug delivery.

MNs-mediated transdermal drug delivery requires 1) the material to have sufficient mechanical strength to penetrate the skin barrier; 2) the material to be biocompatible and not to cause irritation or other immune reactions after the application; 3) the material to be dissolved or bio-degraded while releasing its payload;[8] 4) the release profile of the drug to be slow and uniform to provide a sustained release for extended period of time. From a drug release perspective, MNs can be classified as dissolvable, swellable, and biodegradable MNs.[9] The characteristics of the MN polymer and solvent used, including solubility, molecular weight, viscosity, concentration, and air content, would significantly affect the mechanical strength, stability, drug loading and release profiles of MNs.[10] Selection of MN material and specific fabrication method would determine the mode and rate of drug release from polymer matrices[11]. Because of the high biocompatibility and biodegradability, hydrogels have been adopted in fabricating MNs. The hydrogels can be roughly divided into two types: 1) natural hydrogels, such as cellulose,[2b, 12] hyaluronic acid,[13] chitosan,[14] gelatin,[15] and alginate;[16] and 2) synthetic hydrogels, such as acrylate polymers,[17] poly (β-ester),[18] polylactide,[11] polyvinyl alcohol,[19] and polyvinylpyrrolidone[20]. Natural hydrogel-based MNs usually possess innate biocompatibility and biodegradability and they have been applied to deliver a variety of drugs, ranging from small molecules to biomacromolecules. Although natural hydrogel-based MNs can deliver almost all kinds of drugs in active form, it is still challenging to deliver drugs in a sustained manner.[21] On the other hand, synthetic hydrogel-based MNs can be easily modified for desired drug release behaviors but they are generally less biocompatible than natural hydrogels. It is highly desirable to combine the merits of natural and synthetic hydrogels and to investigate novel materials with innate biocompatibility and biodegradability for the generation of MNs with sustained drug release profiles. GelMA, which is a derivative of gelatin with modified methacrylamide or methacrylate groups, would be an ideal candidate.[22]

GelMA is originated from natural hydrogel gelatin and could be crosslinked by ultra-violet (UV) or visible light in the presence of photo-initiators.[23] It is a highly biocompatible material that is commonly used to support cell growth in tissue engineering.[24] The existence of peptide moieties like arginine-glycine-aspartic acid (RGD) for cell attachment as well as for protease degradation makes GelMA a close mimic of the natural extracellular matrix (ECM).[25] In the meantime, GelMA is a versatile material that can be easily

functionalized with various bio-functionalities, such as by encapsulating different molecules including drugs, growth factors, and cytokines.[22, 26] It was engineered as an injectable material for the delivery of cells in a minimally invasive manner.[27] It has also been developed as a printable bio-ink in the 3D printing of implants, where the GelMA scaffold was found to cause negligible antigenicity.[28] Considering the versatile properties of GelMA, we expect that GelMA could be a promising material to make MNs for sustained drug release.

In this study, we developed a transdermal drug delivery system using GelMA as a major material (Figure 1). The MN patches were fabricated by micro transfer molding and the anticancer drug DOX was loaded by one step molding, and crosslinked by UV irradiation. We evaluated the mechanical properties and drug release behaviors of the DOX-loaded MNs. The efficacy of the DOX released from the GelMA MNs was demonstrated using a melanoma cell line A375.

As shown in Figure 1, the GelMA solution containing DOX was cast into a micro-mold with the 11×11 array. After crosslinking by UV irradiation, the MNs patch was solidified by drying. As shown in Figure 2, an array of MNs with sharp tips was fabricated from GelMA by the micro-mold casting method. While drug-free MNs exhibited a white color (Figure 2a), after loading with DOX, the MNs turn to the color pink (Figure 2b). SEM shows the detailed dimensions of the prepared MNs with a height around 600 μm and a base width of around 300 μm (Figure 2c). Yan et al. evaluated the effect of MN lengths (ranging from 100 μm to 1100 μm) on the penetration to skin. They found that the length of 600 μm was optimal to penetrate skin barrier and prevent the skin wrapping effect. Further increase of MN length (greater than 600 μm) did not show significant improvement for drug delivery. [29] By covalently modifying the GelMA with FITC, DOX encapsulation in the MNs was further characterized by fluorescent microscopy. As shown in Figure 2d, DOX was evenly distributed in the MNs and the MNs bases.

GelMA is hydrophilic porous material that is often applied in the form of a hydrogel. Applying the MNs onto the skin could lead to absorption of interstitial fluids into the MNs. Swelling of the MNs could facilitate the release of the payload, and also has the potential to enhance the interaction of the MNs with the inserted cavity, stabilizing them into the punctured site. To investigate the effect of fluids on the swelling behavior of GelMA MNs, we used DPBS to simulate the body fluid and tested the swelling ratio of GelMA MNs. As shown in Figure 3a, GelMA MNs with different crosslinking degrees all showed a swelling ratio of over 200%. Interestingly, extended crosslinking time resulted in a higher swelling ratio. This could be due to the relatively high solubility of GelMA MNs with low crosslinking degrees, where faster dissolution of GelMA caused higher weigh loss after 24 h incubation in DPBS. We next used confocal microscopy to observe the swelling of GelMA MNs (Figure 3b). It was observed that the swelling ratio reduced the height of the MNs and increased their width. The unique formulation of GelMA-MNs means that the structures have the ability to absorb interstitial flids from the skin upon insertion and swell. The drug release rate can be adjusted by controlling the degree of polymer cross-linking. After the initial application as a tool to penetrate the *stratum corneum* barrier, the MNs become a rate controlling membrane. In order to better understand the structural stability of MNs, the

morphology of repeatedly swelled and deswelled MNs was imaged and shown in Figure 3c. After 5 cycles of swelling and deswelling, the MNs showed partial loss of the mass but the rough MNs structure still remained. Since it is unlikely that one MN patch will be used repeatedly, the structural collapse after repeated swelling and deswelling will not compromise the drug delivery.

We next characterized the mechanical strength of the GelMA MNs, which is an important factor affecting the capability of the MNs to penetrate skin. MNs arrays formulated using the super swelling formulation, with an 11×11 array were used to investigate the effects of compression tests on the heights of the individual needles in the MNs array. As shown in Figure 3d, materials with higher crosslinking density required a higher amount of force to generate the same amount of compression, indicating that the increase of crosslinking time can significantly improve the mechanical strength of MNs. Therefore, the amount of crosslinking in the GelMA microneedle is an important parameter in determining the mechanical properties of the microneedles.

Besides swelling induced porosity of the GelMA MNs, enzymatic degradation is another major factor in controlling the rate of drug release. To investigate protease-mediated degradation of GelMA and its associated effect on drug release, we incubated GelMA MNs in a collagenase solution. Changes in the wet weight of GelMA MNs were recorded to calculate the degradation rate of the MNs. As shown in Figure 4a, GelMA MNs crosslinked for 15 s rapidly degraded within 6 h (70%), while GelMA MNs with high crosslinking degree (60 s) showed only 20% of degradation after 24 h.

Furthermore, we tracked the amount of released DOX from the GelMA MNs by testing DOX fluorescence in the supernatant of the solution incubated with DOX-MNs while being in the presence of the protease. The release kinetics of DOX from MNs were assessed over a period of 24 h. Figure 4b shows that the higher crosslinking time resulted in decreased release rates. MNs without crosslinking released over 80% of DOX in 30 min, while only a quarter of DOX was released in MNs that were crosslinked for 60 s. After being crosslinked for 60s, MNs showed ~ 50% release of the encapsulated DOX within the first 2 h, and then the remaining 20% was slowly released in the next 22 h, indicating that the DOX needed much more time to diffuse from crosslinked MNs. The possible reason was that the porous structure of GelMA MNs became much compact after crosslinking, which trapped DOX inside the crosslinked network of MNs. As time went by, MNs patches were gradually degraded by enzymolysis, and then the trapped DOX was subsequently released. Consequently, the lower release rate of DOX from crosslinked MNs could reduce the risk of cytotoxicity.

After investigating the mechanical properties of GelMA MNs, we further tested the ability of the MNs to penetrate skin in a mouse cadaver skin model. Mouse cadaver skin is widely used as a model for *in vitro* skin drug delivery studies,[30] where the skin structure and permeability of the animal resemble that of humans. Compared with untreated skin (Figure 5a), the MNs-treated skin showed an 11×11 array of microchannels (Figure 5b). To help visualize the micro-punctures, we stained the treated skin with trypan blue, which is a dye that preferably binds to damaged cells (Figure 5c). This observation indicated a 100%

penetration efficiency of MNs into rat skin. As shown in Figure 5d, the surface of the untreated mouse cadaver skin was smooth and is composed of epidermis, dermis, and hypodermis. Recurring microcavities with a depth of 400~600 μm can be observed after the insertion of MNs (Figure 5e). After 5 min of insertion, the interstitial fluid of the mouse cadaver skin was absorbed by MNs and resulted in the swelling of the MNs. In spite of their swelling, the MNs retained their mechanical toughness in the hydrated state, which enabled their removal from the skin in an intact manner.

We next confirmed that the UV mediated crosslinking process and the enzyme-mediated digestion of the GelMA scaffold did not influence the anticancer activity of the loaded DOX. We used a human melanoma cell line A375 as the model to investigate the anticancer efficiency of DOX released from the MNs. After incubating MNs containing 10 μg of DOX with the plated cells for 1 h, the viability of A375 cells was examined using an MTT assay after 24 h. As shown in Figure 6a, a reverse correlation between cell viability and crosslinking time was observed, which was in agreement with the fact that extended crosslinking times resulted in denser GelMA and reduced DOX release rates. The DOX-induced cell death was further investigated by a Live/Dead assay, where live cells metabolized calcein AM into the green fluorescent calcein, and dead cells with compromised membrane integrity were stained by the red fluorescent dye EthD-1. As shown in Figure 6b to 6f, the cell death was observed in the DOX-treated cells. In addition, A375 cells treated by crosslinked MNs were observed less cell death than those treated by uncrosslinked MNs, which was correlated with the viability assay (Figure 6a). The possible reason was that MNs with more crosslinking time would release less DOX at the same releasing time (1 h).

Microneedle technology is promising for transdermal delivery of therapeutic drugs since it enables drugs to pass through the *stratum corneum* via microchannels in a minimally invasive manner.[31] In general, the characteristics of the polymer and the casting medium can highly influence the properties of the microneedles. In this study, we used GelMA as the base material to fabricate MNs, and demonstrated their use for transdermal drug delivery by showing their skin penetration capability as well as the preservation of the therapeutic activity of the drug after release. The mechanical and material characteristics of GelMA MNs can be easily modulated by controlling their crosslinking degrees. Varying the crosslinking time (0 s to 60 s), the swelling ratio was found to change from about 250% to 290% (Figure 3a **and** 3b) and the mechanical strength was greatly enhanced (Figure 3d). Compared with GelMA MNs with a low crosslinking degree, the degradation rate of GelMA MNs crosslinked for 60 s was sharply reduced, and the drug release profile was well controlled by varying the crosslinking time (Figure 4a **and** b). Since the *in vitro* drug release test set-up in this study contained a greater amount of water than the actual skin tissue, releasing drugs could be faster than *in vivo* conditions, but the overall release profile should be similar. GelMA has been verified for its biocompatibility by being widely used in applications ranging from the food industry [32] to medicine and pharmaceutical processing. [33] This material has also shown superior cell viability for a wide range of cells. [34] *In vitro* and in vivo studies with GelMA have shown that that GelMA hydrogels supported functional cell growths and promoted tissue healing with stable biocompatibility in animal

models.[35] The degradation characteristic of GelMA have been already confirmed in various ways.[34] In light of this, GelMA MN has strengths in that it leaves no hazardous materials after biodegradation of GelMA.

MNs patches for transdermal delivery are currently being explored in the forms of hollow, coated and dissolvable MNs.[10, 36] Among them, the majority of MNs patches tend to be coated un-dissolvable MNs or dissolvable MNs. During the earlier days of MNs research, transdermal MNs were coated with the desired drugs using a dip-coating approach and the drug formulations included the target drug, surfactant, and viscosity enhancer.[37] This drug formulations were usually coated onto the MNs consisting of robust materials such as metal or silicon. With these coated MNs, the drugs were delivered across the skin barrier in small amounts, where the MNs have limited drug loading capacity. In addition, the drug transfer mechanism from MNs to the inner skin tissue is still not well understood, and there is a possibility that the delivered drug could be lost through the open space of MNs insertion mark. The dissolving MNs can overcome the limitations of drug loading capacity compared to the coated MNs but has the same potential drug loss like in the case of coated MNs due to incomplete insertion or dissolving of MNs.[38] Separable arrowhead MNs could be an alternative to prevent drug loss to fully embed the drug-loaded arrowhead in the skin.[39] In addition, the microlancer integrated dissolving MNs, which is a micropillar based system, was shown to achieve $97 \pm 2\%$ delivery efficiency by fully embedding the MNs with the aid of microlancer.[40] However, sustained drug delivery has not been demonstrated by the current dissolving MNs. On the other hand, GelMA MNs consisting of a mechanically enhanced hydrogel containing DOX can penetrate across *stratum corneum* and reach the desired depths of the skin later. It is noteworthy to mention that GelMA MNs released their DOX cargo for a sustained period (up to 24 hrs.) and the delivery was carried out as the material slowly biodegraded at a slow pace. There have been several attempts to achieve sustained drug delivery in the dissolving MNs platform. A platform having encapsulated molecules within the microneedles which dissolved within the skin for bolus or sustained delivery was reported.[21a] Lysozymes were encapsulated with sulforhodamine B and molded with carboxymethyl cellulose mixture for creating dissolvable MNs. This design provided drug release for 9 hrs. Drug-loaded biodegradable poly(lactic-co-glycolic) acid (PLGA) microparticles in water-soluble poly(acrylic acid) (PAA) MNs matrix was developed for long-term drug release.[41] Another representative study introduced an embeddable chitosan MNs onto supporting array for sustained delivery of encapsulated antigens to the skin.[31] This chitosan MNs exhibited a sustained release of encapsulated antigens for up to 7 days in vitro via slow degradation. These representative dissolving MNs for sustained drug delivery demonstrated controllable release profiles or long-lasting drug residue within the skin tissue, but additional fabrication steps including drug encapsulation or inclusion of particles are needed which makes the process unnecessarily complicated. However, GelMA MNs can be easily loaded drugs by a simple mixing procedure, release the drug for a certain period by simply modulating the degree of crosslinking. Also, when the GelMA MNs patch is applied to the tissue, there is no risk of drug loss because the substrate of GelMA MNs patch covers top of the tissue until MN delivers the drug.

In this study, we demonstrated GelMA as a promising material for the fabrication of a dissolvable MNs that can be used to deliver anticancer therapeutics. We demonstrate that dry

GelMA based MNs exhibited sufficient mechanical strength to penetrate into mouse cadaver skin, and the MNs did not break or bend after the insertion. The GelMA MNs released their loaded therapeutics through both swelling and enzymatic degradation of the scaffold. Compared with burst release that is often observed in some micro-needle formulations, the GelMA based MNs patch exhibited a gradual release of the loaded DOX, especially at higher crosslinking degrees (30 s and above). The controlled release was able to reduce the concern for burst release resultant toxicity. At high crosslinking degrees, a linear sustained release of DOX from the MNs was observed as oppose to a burst release. The DOX-loaded MNs has immense potential to function as a minimally invasive therapy for transdermal treatment of melanoma. As a versatile material in engineering tissue scaffolds, GelMA is also expected to be a promising platform for the delivery of both small molecule drugs and bio-macromolecular drugs including proteins, nucleic acids even cells.

Experimental Section

GelMA preparation:

GelMA was prepared as previously described.[22] Briefly, 10 g of type A porcine skin gelatin was added into 100 mL of DPBS preheated to 60 °C under constant stir. Methacrylic anhydride (8 mL) was gradually added and the reaction was kept under vigorous stirring for 3 h at 50 °C. The reaction was stopped by adding a 5-fold volume of warm DPBS (40 °C). Residual salts and methacrylic anhydride were removed by dialysis in distilled water at 40 °C for 1 week using dialysis tubing with molecular weight cut-off of 12-14 kDa. After lyophilization for one week, GelMA in the form of white porous foam was obtained, which was stored at −20 °C for further use. FITC conjugated GelMA was obtained as follows: 1 g of GelMA was dissolved in 30 mL of DPBS and 0.1% FITC were mixed and the mixture was then reacted at 40 °C for 24 h in darkness, the conjugate was then dialyzed using dialysis tubing with a molecular weight cut-off of 12-14 kDa in distilled water at 40 °C. The FITC modified GelMA in the form of yellow porous foam was obtained after lyophilization and was stored in darkness.

Preparation of DOX-loaded GelMA MNs:

For the MNs preparation, 0.4 g of GelMA was dissolved in 1.5 mL of DPBS solution at 50 °C. Then 0.5 mL of DOX (400 μg mL^{-1}) and 10 mg of photoinitiator (Irgacure 2959) were added to the solution at 50 °C under vigorous stirring. The MNs mold was immersed into the prepolymer solution and sonicated for 1h at 40 °C, and then taken out of the solution and exposed to 350 mW (cm^2)$^{-1}$ UV light (360-480 nm) for predefined exposure durations (0, 15, 30 and 60 s). The resulting MNs were manually removed from the mold after being dried in the dark for 24 h at room temperature.

Mechanical properties of MNs:

The mechanical strength of MNs was measured under dynamic force using a stress-strain gauge. The MN array was pressed against a stainless-steel plate on a low-force mechanical testing system (5943 MicroTester, Instron, USA), correlations between the applied force and deformation of the MNs were recorded. Initially, the MNs tips was placed perpendicularly to stainless steel plate with a 1.5 mm distance and the maximum loading force was set at 50.0

N. Under a constant moving speed of stainless-steel plate (0.5 mm min^{-1}), the mechanical properties of MNs with different crosslinking times (0, 15, 30 and 60 s) were profiled. All tests were performed in triplicate.

Swelling, enzymatic degradation and drug release profile of DOX-MNs:

To analyze the swelling of the DOX-MNs, UV crosslinked MNs patches were incubated in DPBS for 24 h at 37 °C. Incubated MNs were blotted to remove residual liquids, wet weight (W_w) of the MNs were recorded after MNs reached the equilibrium of swelling. The dry weights (W_d) were measured after freeze-drying. The swelling ratio was calculated as [(W_w-W_d)/W_d]×100%. Three samples were used for the measurements to calculate the mean and standard deviations. The structural stability of MNs was next investigated. MNs crosslinked for 60s were placed into a DPBS solution and swelled for 60 min, and then the samples were retrieved and dried in vacuum. The swelling and deswelling procedures were repeated for 5 times, and then the morphology of the obtained samples was checked with SEM. *In vitro* degradation of MNs was also analyzed. MNs were immersed in DPBS (5 mL) containing collagenase type Ⅱ (2 U mL^{-1}) and incubated at 37 °C. At the pre-determined time points, MNs were retrieved from the solution and the wet weights were recorded after blotting. The degradation ratio of MNs was calculated as (W_t/W_0)×100% (where W_t is residual wet weight at different time points and W_0 is the initial wet weight).[42] All experiments were performed in triplicate. To investigate the drug release profiles of the MNs, dried MNs loaded with DOX were immersed into 5 mL DPBS containing collagenase type Ⅱ (2 U mL^{-1}). The samples were kept at 37 °C, 100 μL of the DPBS was sampled at predefined time points, and the fluorescence of DOX (excitation 480 nm, emission 560 nm) was read using a Plate Reader (BioTek, USA). After the measurements, each sample was returned to the solution for drug release analysis. DOX was quantified using a calibration curve of DOX solutions with known concentrations (0.005~5 μg mL^{-1}).

Skin penetration by the MNs:

To examine whether the MNs are mechanically strong enough to penetrate the skin, a mouse cadaver skin model was used. A MNs patch was pushed into the mouse cadaver skin by a compression force station (Instron, USA) with a force of 20 N for 5 s. Trypan blue, a dye that could stain damaged cell membranes, was then used to stain the penetrated tissue for 5 min. After removing excess trypan blue, the skin was imaged using an optical microscope (Zeiss, Sweden) to check for the sign of penetrating *stratum corneum* (blue dots). The cadaver skin of a mouse with MNs inserted was freshly frozen in OCT compound, and 10 μm thick cross-sectional slices were visualized on the Zeiss Axio Observer Z1 microscope (Carl Zeiss, Germany).

In vitro anticancer efficacy of the released DOX:

In vitro cytotoxicity of the released DOX was evaluated using the melanoma cell line A375 as the model. Specifically, A375 cells were plated in 24-well plates (1×10^6 per well) and incubated for 24 h. MNs with different crosslinking degrees were added and incubated for 1 h. After that, the MNs were removed from the wells, and A375 cells were incubated for another 24 h. The effects of DOX on the metabolic activity of A375 cells *in vitro* were tested with a rapid colorimetric MTT assay. The absorbance of the wells was read at 570 nm with

630 nm as the reference. Live/dead staining was performed to visualize the viability of A375 cells after treatment with DOX released from the MNs. The stained cells were then imaged by a fluorescent microscope (Zeiss, Sweden).

Statistical analysis:

At least three independent sets of experiments for each condition were performed in triplicate. We did the analyses with the Origin 8.0 software. All data were pooled and statistically expressed as the mean $\pm$ standard deviation (S.D.). Two-tailed Student's t-test was carried out to evaluate the significance of the experimental data. Statistics was considered significant when $p < 0.05$ or less.

Acknowledgments

References

[1]. Kanitakis J, Eur. J. Dermatol 2002, 12, 390. [PubMed: 12095893]

[2]. a) Jepps OG, Dancik Y, Anissimov YG, Roberts MS, Adv. Drug Deliver. Rev 2013, 65, 152;b) Lee C, Kim H, Kim S, Lahiji SF, Ha NY, Yang H, Kang G, Nguyen HYT, Kim Y, Choi MS, Cho NH, Jung H Adv. Healthc. Mater 2018, 7, e1701381. [PubMed: 29663698]

[3]. Gill HS, Denson DD, Burris BA, Prausnitz MR, Clin. J. Pain 2008, 24, 585. [PubMed: 18716497]

[4]. Prausnitz MR, Mitragotri S, Langer R, Nat. Rev. Drug Discov 2004, 3, 115. [PubMed: 15040576]

[5]. Prausnitz MR, Annu. Rev. Chem. Biomol. Eng 2017, 8, 177. [PubMed: 28375775]

[6]. Yu J, Zhang Y, Ye Y, DiSanto R, Sun W, Ranson D, Ligler FS, Buse JB, Gu Z, Proc. Natl. Acad. Sci. U. S. A 2015, 112, 8260; Fakhraei Lahiji S, Seo SH, Kim S, Dangol M, Shim J, Li CG, Ma Y, Lee C, Kang G, Yang H, Choi KY, Jung H, Biomaterials 2018, 167, 69. [PubMed: 26100900]

[7]. Jenning V, Gysler A, Schäfer-Korting M, Gohla SH, Eur. J. Pharm. Biopharm 2000, 49, 211. [PubMed: 10799811]

[8]. Ramot Y, Haim-Zada M, Domb AJ, Nyska A, Adv. Drug Deliver. Rev 2016, 107, 153.

[9]. Demir YK, Akan Z, Kerimoglu O, PloS One 2013, 8, e77289. [PubMed: 24194879]

[10]. Kim Y-C, Park J-H, Prausnitz MR, Adv. Drug Deliver. Rev 2012, 64, 1547.

[11]. Kim M, Jung B, Park J-H, Biomaterials 2012, 33, 668. [PubMed: 22000788]

[12]. Ribeiro AM, Magalhães M, Veiga F, Figueiras A, Cellulose-Based Superabsorbent Hydrogels 2018, 1.

[13]. Larrañeta E, Henry M, Irwin NJ, Trotter J, Perminova AA, Donnelly RF, Carbohyd. Polym 2018, 181, 1194.

[14]. Chen M-C, Ling M-H, Lai K-Y, Pramudityo E, Biomacromolecules 2012, 13, 4022. [PubMed: 23116140]

[15]. Ling M-H, Chen M-C, Acta Biomater 2013, 9, 8952. [PubMed: 23816646]

[16]. Chen X, Corbett HJ, Yukiko SR, Raphael AP, Fairmaid EJ, Prow TW, Brown LE, Fernando GJ, Kendall MA, Adv. Funct. Mater 2011, 21, 464.

[17]. Qiu Y, Qin G, Zhang S, Wu Y, Xu B, Gao Y, Int. J. Pharmaceut 2012, 437, 51.

[18]. Mikolajewska P, Donnelly RF, Garland MJ, Morrow DI, Singh TRR, Iani V, Moan J, Juzeniene A, Pharm. Res 2010, 27, 2213. [PubMed: 20676735]

[19]. Lee I-C, He J-S, Tsai M-T, Lin K-C, J. Mater. Chem. B 2015, 3, 276.

[20]. Sullivan SP, Koutsonanos DG, del Pilar Martin M, Lee JW, Zarnitsyn V, Choi S-O, Murthy N, Compans RW, Skountzou I, Prausnitz MR, Nat. Med 2010, 16, 915. [PubMed: 20639891]

[21]. a) Lee JW, Park J-H, Prausnitz MR, Biomaterials 2008, 29, 2113; [PubMed: 18261792] b) Thote AJ, Chappell JT, Kumar R, Gupta RB, Drug Dev. Ind. Pharm 2005, 31, 43; [PubMed: 15704857] c) Wang C, Ye Y, Hochu GM, Sadeghifar H, Gu Z, Nano Lett 2016, 16, 2334. [PubMed: 26999507]

[22]. Yue K, Trujillo-de Santiago G, Alvarez MM, Tamayol A, Annabi N, Khademhosseini A, Biomaterials 2015, 73, 254. [PubMed: 26414409]

[23]. Zhao X, Lang Q, Yildirimer L, Lin ZY, Cui W, Annabi N, Ng KW, Dokmeci MR, Ghaemmaghami AM, Khademhosseini A, Adv. Healthc. Mater 2016, 5, 108. [PubMed: 25880725]

[24]. Xavier JR, Thakur T, Desai P, Jaiswal MK, Sears N, Cosgriff-Hernandez E, Kaunas R, Gaharwar AK, ACS Nano 2015, 9, 3109. [PubMed: 25674809]

[25]. Liu Y, Chan-Park MB, Biomaterials 2010, 31, 1158. [PubMed: 19897239]

[26]. Yetisen AK, Butt H, Volpatti LR, Pavlichenko I, Humar M, Kwok SJ, Koo H, Kim KS, Naydenova I, Khademhosseini A, Hahn SK, Yun SH, Biotechnol. Adv 2016, 34, 250. [PubMed: 26485407]

[27]. Noshadi I, Hong S, Sullivan KE, Shirzaei Sani E, Portillo-Lara R, Tamayol A, Shin SR, Gao AE, Stoppel WL, Black LD III, Khademhosseini A, Annabi N, Biomater Sci 2017, 5, 2093. [PubMed: 28805830]

[28]. Annabi N, Shin SR, Tamayol A, Miscuglio M, Bakooshli MA, Assmann A, Mostafalu P, Sun J-Y, Mithieux S, Cheung L, Tang X, Weiss AS, Khademhosseini A, Adv. Mater 2016, 28, 40. [PubMed: 26551969]

[29]. Yan G, Warner KS, Zhang J, Sharma S, Gale BK, Int. J. Pharmaceut 2010, 391, 7.

[30]. Bronaugh RL, Stewart RF, Congdon ER, Toxicol. Appl. Pharm 1982, 62, 481.

[31]. Chen M-C, Huang S-F, Lai K-Y, Ling M-H, Biomaterials 2013, 34, 3077. [PubMed: 23369214]

[32]. Gómez-Guillén MC, Giménez B, López-Caballero ME, Montero MP, Food Hydrocolloid 2011, 25, 1813.

[33]. Djagny VB, Wang Z, Xu S, Crit. Rev. Food Sci 2001, 41, 481.

[34]. Yue K, Trujillo-de Santiago G, Alvarez MM, Tamayol A, Annabi N, Khademhosseini A, Biomaterials 2015, 73, 254. [PubMed: 26414409]

[35]. Noshadi I, Hong S, Sullivan KE, Shirzaei Sani E, Portillo-Lara R, Tamayol A, Shin SR, Gao AE, Stoppel WL, Black Iii LD, Khademhosseini A, Annabi N, Biomater. Sci 2017, 5, 2093. [PubMed: 28805830]

[36]. a) Hirobe S, Azukizawa H, Hanafusa T, Matsuo K, Quan YS, Kamiyama F, Katayama I, Okada N, Nakagawa S, Biomaterials 2015, 57, 50; [PubMed: 25913250] b) Matsuo K, Okamoto H, Kawai Y, Quan YS, Kamiyama F, Hirobe S, Okada N, Nakagawa S, J. Neuroimmunol 2014, 266, 1. [PubMed: 24315156]

[37]. Gill HS, Prausnitz MR, Control J. Release 2007, 117, 227.

[38]. a) Sullivan SP, Koutsonanos DG, del Pilar Martin M, Lee JW, Zarnitsyn V, Choi S-O, Murthy N, Compans RW, Skountzou I, Prausnitz MR, Nat. Med 2010, 16, 915; [PubMed: 20639891] b) P SS, N M, R PM, Adv. Mater 2008, 20, 933. [PubMed: 23239904]

[39]. Chu LY, Prausnitz MR, Control J. Release 2011, 149, 242.

[40]. Lahiji SF, Dangol M, Jung H, Sci. Rep 2015, 5, 7914. [PubMed: 25604728]

[41]. DeMuth PC, Garcia-Beltran WF, Ai-Ling ML, Hammond PT, Irvine DJ, Adv. Funct. Mater 2013, 23, 161. [PubMed: 23503923]

[42]. Guo J, Liu X, Jiang N, Yetisen AK, Yuk H, Yang C, Khademhosseini A, Zhao X, Yun SH, Adv. Mater 2016, 28, 10244. [PubMed: 27714887]
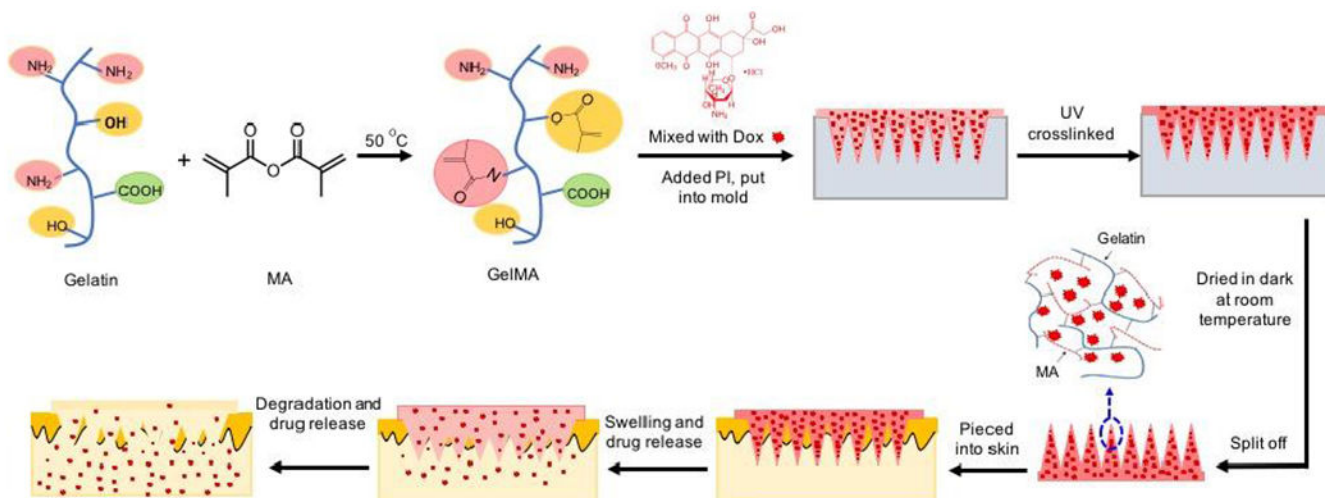
Figure 1.
Schematic of the GelMA MNs for sustained drug delivery. Gelatin was modified with MA to generate GelMA polymers, then DOX was mixed with the GelMA prepolymer solution and casted into the micro molds. DOX-loaded GelMA MNs were then crosslinked by UV irradiation. After drying and curing, the MNs were peeled off from the micromold. The dissolvable MNs are sharp enough to penetrate the skin barrier and are degradable, and MNs can have the ability to release the loaded DOX into the transdermal space.
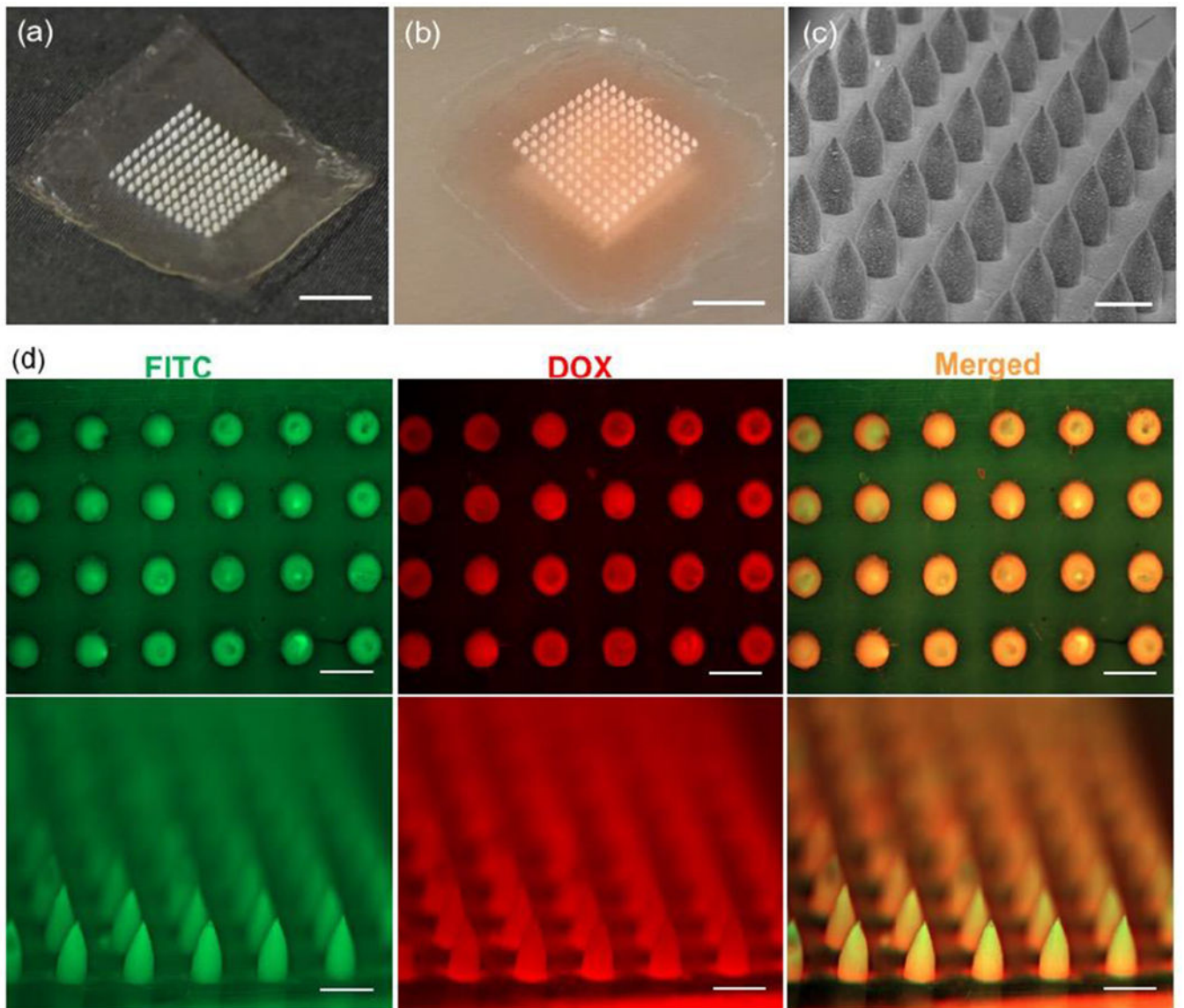

Figure 2.
Morphological characterization of the DOX-loaded MNs. a) Optical images of the GelMA MNs, and scale bar is 5 mm. b) Optical image of DOX-loaded MNs, and scale bar is 5 mm. c). SEM image of the GelMA MNs, and scale bar is 500 μm. d) Fluorescent microscope image of DOX-loaded GelMA MNs. Green represents FITC modified GelMA, red represent DOX. Scale bars are 500 μm.
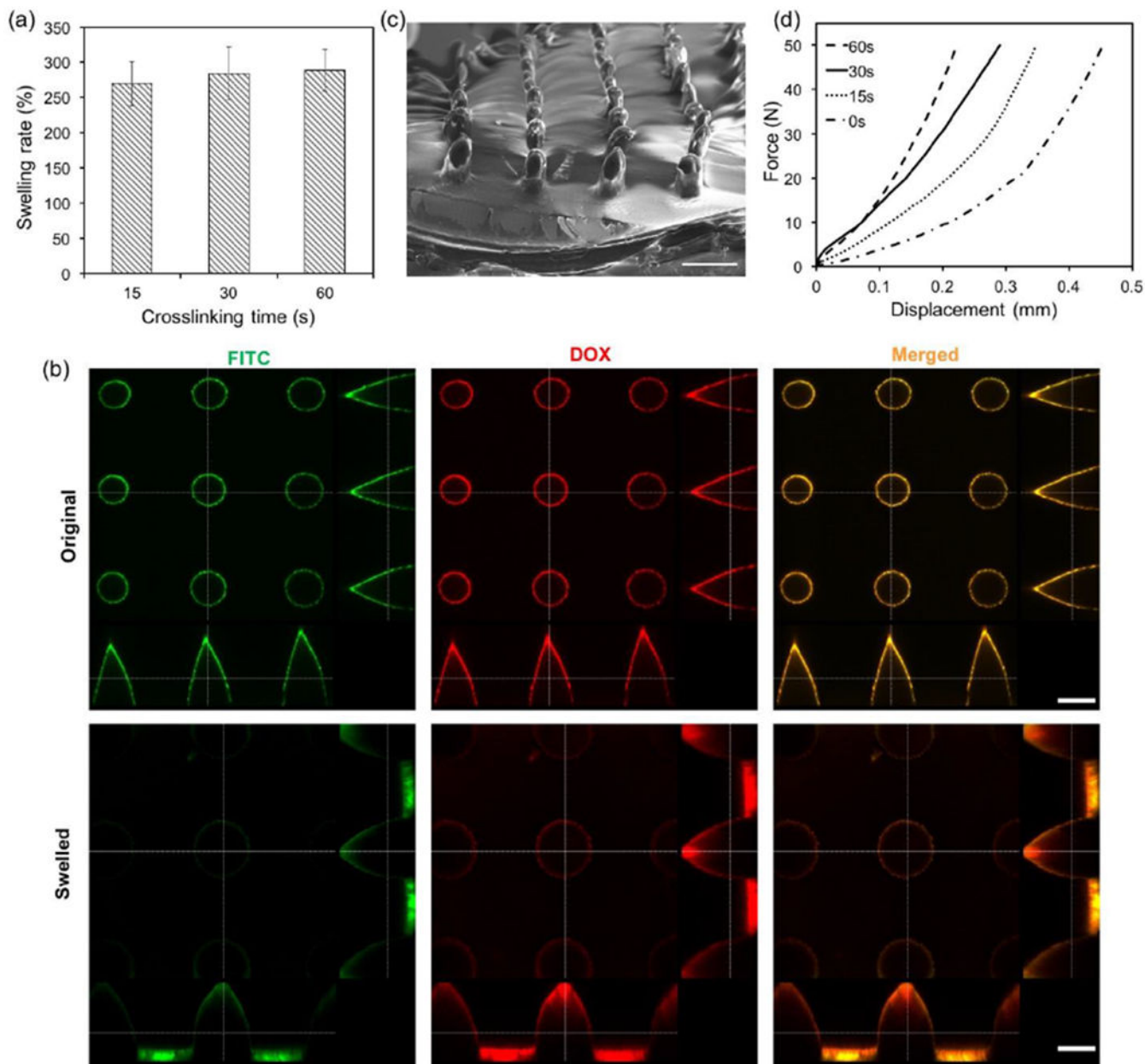
Figure 3.
Characterization of the mechanical properties of DOX-loaded GelMA MNs. a) Effect of crosslinking time on swelling rate. The error bars represent S.D. (n=3). b) Representative swelling of the DOX-loaded MNs. The MNs was scanned by CLSM, green represents FITC modified GelMA, red represents DOX, and scale bars are 250 μm. c) SEM image of MNs crosslinked for 60 s after 5 cycles of swelling and deswelling, and scale bar is 500 μm. d) Effect of the duration of crosslinking on mechanical strength of the MNs.
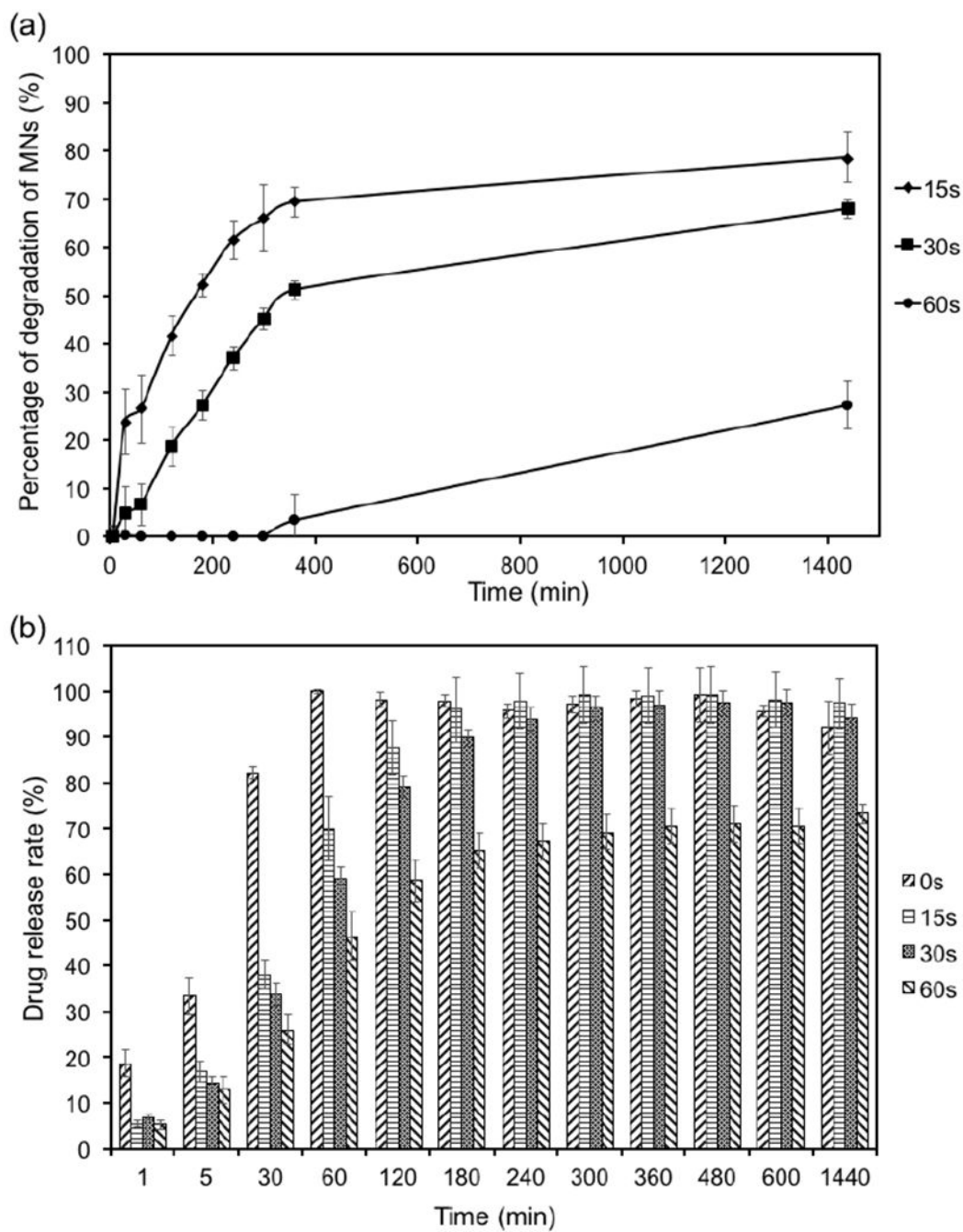
Figure 4.
Enzymatic degradation of the MNs and drug release. a) The effect of the crosslinking time (15, 30 and 60s) on enzymatic degradation rate. The error bars represent S.D. (n=3). b) The effect of crosslinking time on the release of DOX from GelMA MNs. The error bars represent S.D. (n=3).
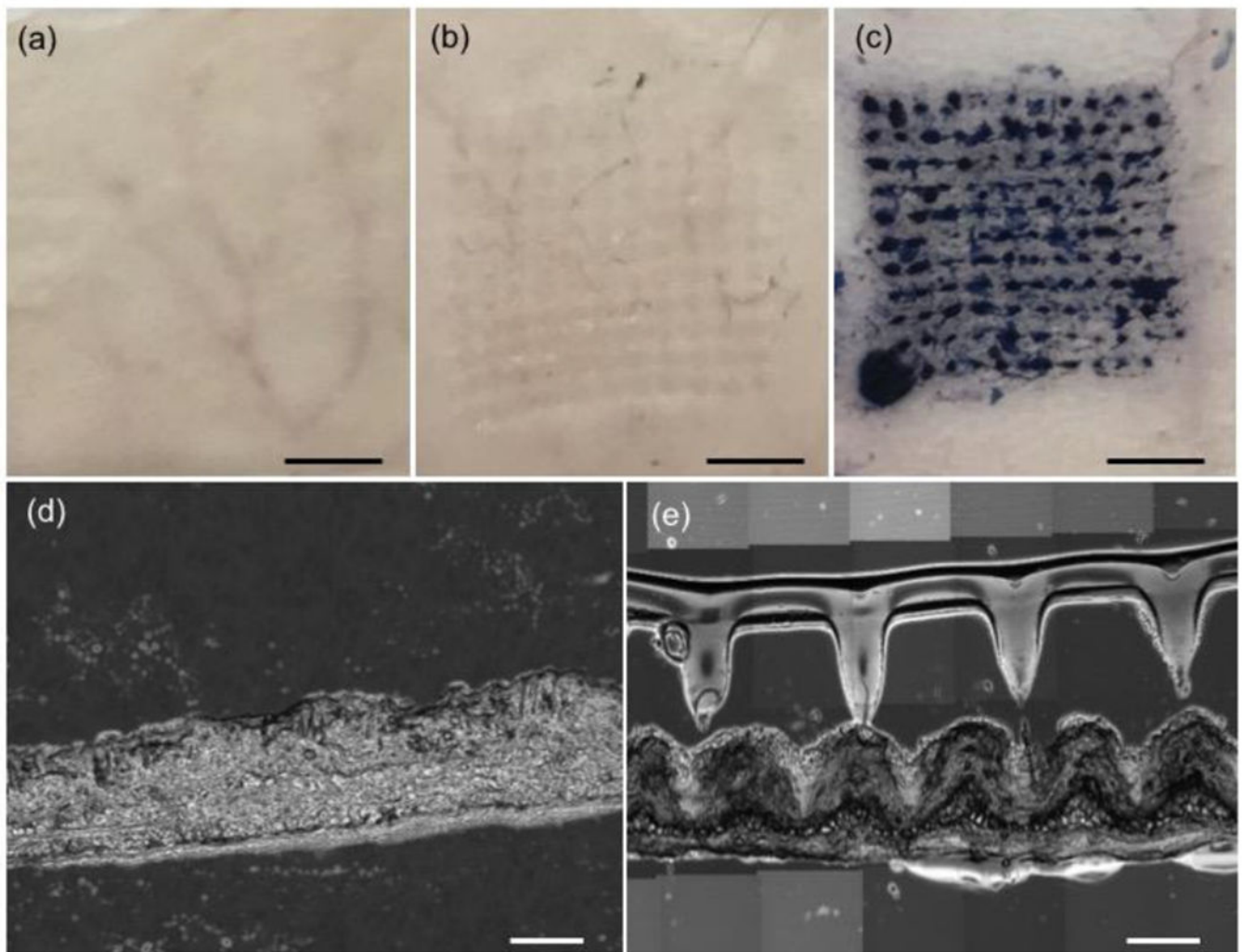
Figure 5:
Penetration of the mouse cadaver skin by the GelMA MNs. Trypan blue staining of the penetrated skin: (a) untreated control, (b) skin treated with MNs only, (c) skin treated with MNs after Trypan Blue staining, and scale bars are 2 mm; Optical microscopy images of normal mouse skin before (d) and after (e) treating with MNs for 5 min, and scale bars are 500 μm.
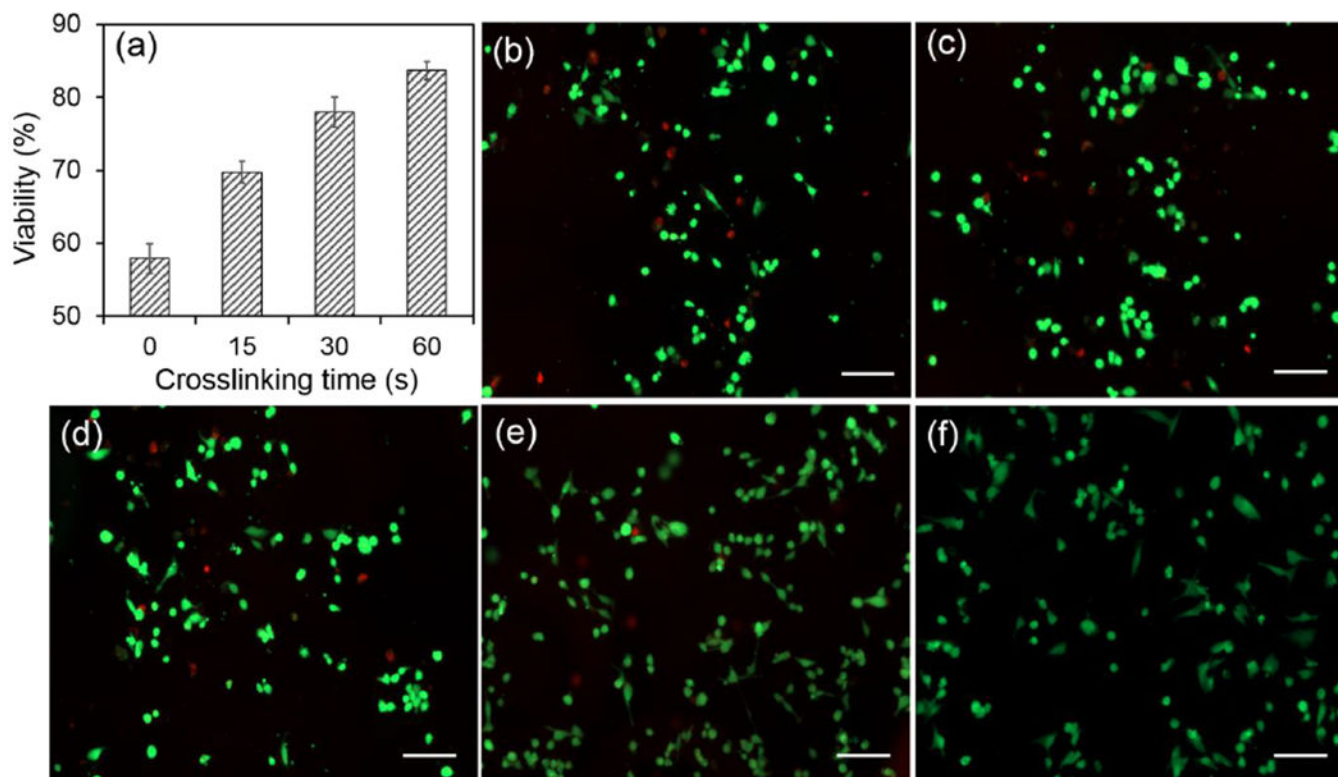
Figure 6:
In vitro cytotoxicity study of the efficacy of DOX released from the MNs patch. (a) Melanoma cell line A375 was used as the model cell line, where the cell viability was examined by the MTT assay. Effect of crosslinking time on cell viability was studied. Error bar represents S.D. (n=3). (b~f) Fluorescent microscopic images of A375 cells treated with different MNs for 1 h (b~e: crosslinking time: 0, 15, 30, 60 s, respectively, f: control cell without DOX treatment), and scale bars are 100 μm. The cells were stained by a Live/Dead assay, green represents live cells and red shows dead cells.